

$J$  induced by conformational changes [200]. Biradicals have also been studied in liquid crystalline solvents, in which they are partially aligned [159]: the dipolar interaction between the spins is not now averaged to zero and from the observed splitting of the lines the zero-field splitting can be obtained. The theory of this section extends quite readily to triradicals and, so far as these have been studied, gives a good description of their spectra [201].

## CHAPTER 6

# THE THEORY OF THE $g$ -TENSOR

### 6.1 Introduction

In Chapter 2 we worked through some qualitative ideas to make it seem reasonable that electron resonances should not always occur at the magnetic field expected for a free electron, and we introduced the  $g$ -tensor and its isotropic component, the  $g$ -factor. We now seek to achieve a deeper understanding of the  $g$ -tensor, establishing the links between this experimentally determined parameter of the spin Hamiltonian and the electronic structure of the system being studied.

The theory of the  $g$ -tensor is generally held to be more difficult than that of the other topics we have covered so far, and we will approach it circumspectly. We will first discuss the method by which the tensor is measured from the spectra of an oriented sample and then go through some explicit calculations for transition metal ions. These should establish the physical nature of the problem, and facilitate the application of the general theory which we will develop in Section 6.5. The advantage of starting with transition metal ions is that there is the simplifying feature that we only consider the electrons on the metal ion itself. This may not sound very relevant to chemists interested in covalent bonding in transition metal complexes but it is best to start with as simple a problem as possible and in any case a crystal field description of a complex often allows the main features of the bonding to be understood reasonably well. The extension of the theory to free radicals will be discussed in Sections 6.5 and 6.7 and covalent bonding in transition metal ion complexes will be discussed in Chapter 7. Finally, in Section 6.8 we will discuss briefly the theory of the  $g$ -tensors of rare-earth metal ions. In these the unpaired electrons occupy  $f$  orbitals and are much more shielded from the environment than are electrons in the  $d$ -orbitals of transition metal ions or the unpaired electron in a free radical. Thus the spin-orbit coupling is relatively more important than the crystal field interaction and it is convenient to modify the calculations somewhat.

### 6.2 Experimental Determination of the $g$ -Tensor

The general principles are similar to those involved in the determination of hyperfine coupling tensors. One studies the spectrum of a magnetically

dilute oriented sample as a function of orientation in the magnetic field, measurements being referred to a set of axes fixed in the crystal [202]. The reference axes, which will not in general be the principal axes of the  $g$ -tensor, will be labelled  $xyz$ .

Consider a radical or ion in a magnetically dilute crystal, and for simplicity assume no hyperfine splitting. The spectrum will then be just a single line whose position in the field will be orientation-dependent. An example might be  $S_2^-$  or  $O_2^-$  in an alkali halide crystal [203], or titanium acetyl acetonate [204]. We assert that the position of the resonance as a function of orientation can be described using the spin Hamiltonian,

$$\mathcal{H} = \beta \mathbf{H} \cdot \mathbf{g} \cdot \mathbf{S} \quad (6.1)$$

and we wish to investigate the eigenvalues of this Hamiltonian and see how to determine the elements of the  $g$ -tensor. If the magnetic field has direction cosines ( $l, m, n$ ) in the reference axis system, and we choose a representation in which  $S_z$  is diagonal in the reference axis system, then the Hamiltonian expands to

$$\begin{aligned} \mathcal{H} = \beta H \{ & S_x(lg_{xx} + mg_{xy} + ng_{xz}) + S_y(lg_{xy} + mg_{yy} + ng_{yz}) \\ & + S_z(lg_{xz} + mg_{yz} + ng_{zz}) \} \end{aligned} \quad (6.2)$$

For a system having  $S = \frac{1}{2}$  the matrix of this Hamiltonian is

$$\begin{array}{cc} |+\frac{1}{2}\rangle & |-\frac{1}{2}\rangle \\ \langle +\frac{1}{2}| & \frac{1}{2}\beta H(lg_{xx} + mg_{xy} + ng_{xz}) & \frac{1}{2}\beta H\{(lg_{xx} + mg_{xy} + ng_{xz}) \\ & & - i(lg_{xy} + mg_{yy} + ng_{yz})\} \\ \langle -\frac{1}{2}| & \frac{1}{2}\beta H\{(lg_{xx} + mg_{xy} + ng_{xz}) & -\frac{1}{2}\beta H(lg_{xz} + mg_{yz} + ng_{zz}) \\ & & + i(lg_{xy} + mg_{yy} + ng_{yz})\} \end{array} \quad (6.3)$$

The eigenvalues are easily calculated, and from the difference between them we find for the  $g$ -factor,

$$g = \hbar\nu/\beta H = \{(lg_{xx} + mg_{xy} + ng_{xz})^2 + (lg_{xy} + mg_{yy} + ng_{yz})^2\}^{1/2} \quad (6.4)$$

It is clear now that the analysis is analogous to that for hyperfine coupling tensors (Sections 4.2, 4.3). For example if the magnetic field is in the  $xy$ -plane, making an angle  $\theta$  with the  $x$ -axis, the  $g$ -factor is

$$g = \{\cos^2 \theta (g_{xy}^2 + g_{xx}^2 + g_{xz}^2) + \sin^2 \theta (g_{yz}^2 + g_{yy}^2 + g_{zy}^2) + 2 \sin \theta \cos \theta (g_{xz}g_{yz} + g_{xx}g_{xy} + g_{yy}g_{xy})\}^{1/2} \quad (6.5)$$

so that the  $xy$ ,  $xx$  and  $yy$  elements of the square of the  $g$ -tensor can be obtained from analysis of the angular dependence of the spectrum in the  $xy$ -plane. The whole procedure parallels that described in Section 4.3, and here we will simply summarise the steps.

- (i) Determine the elements of  $(g^2)$  from rotations about each axis in turn. In cases where there is more than one magnetically distinct site the relative signs of off-diagonal elements can be checked by running a spectrum at a 'skew' orientation.
- (ii) Diagonalise  $(g^2)$ .
- (iii) The square roots of the principal values of  $(g^2)$  are the principal values of  $g$  itself. The problem that all the principal values of the tensor may not have the same sign, which may arise with hyperfine tensors, does not normally arise for  $g$ -tensors. The isotropic component may be extracted as the average of the three principal values.
- (iv) The eigenvectors of  $(g^2)$  give the directions of the principal values of  $g$  in the crystal axis system.
- (v) The  $g$ -tensor in the crystal axis system, which may be useful for predicting spectra in particular orientations, may be obtained from the diagonalised tensor by a suitable rotation.

This procedure is valid for determining the  $g$ -tensors of free radicals and transition metal complexes. Provided the hyperfine splittings are fairly small the  $g$ -factor for a particular orientation is accurately obtained by measuring the position of the centre of the spectrum. However, if the hyperfine splitting is large, so that there is a second or higher order shift (see Section 3.12), then a correction must be applied.

It is quite common to find the spin Hamiltonian written in the principal axis system of the  $g$ -tensor, for example,

$$\mathcal{H} = \beta(g_{xx}H_xS_x + g_{yy}H_yS_y + g_{zz}H_zS_z) \quad (6.6)$$

If the magnetic field has direction cosines ( $l', m', n'$ ) in this axis system, then the observed  $g$ -factor for this orientation is

$$g = (l'^2g_{xx}^2 + m'^2g_{yy}^2 + n'^2g_{zz}^2)^{1/2} \quad (6.7)$$

In many cases there is cylindrical symmetry, when it is usual to define

$$g_{||} = g_{zz}; \quad g_{\perp} = g_{xx} = g_{yy} \quad (6.8)$$

Now if the magnetic field makes an angle  $\theta$  with the symmetry axis, the observed  $g$ -factor is

$$g = (g_{||}^2 \cos^2 \theta + g_{\perp}^2 \sin^2 \theta)^{1/2} \quad (6.9)$$



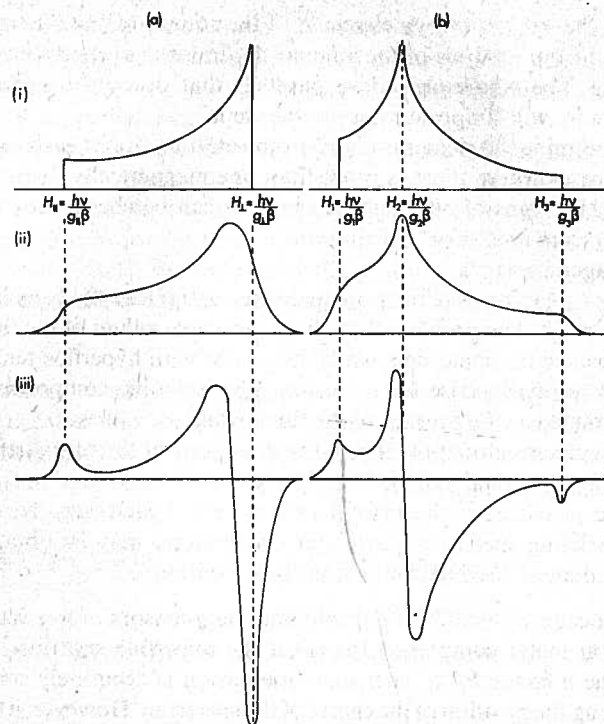


FIG. 6.1. Powder spectra in the case of (a) an axially symmetric, and (b), an orthorhombic  $g$ -tensor. (i) The absorption for an infinitely sharp line, (ii) modification to take account of finite linewidth, (iii) first derivative of (ii).

In cases where the  $g$ -anisotropy is not too small it is often possible to determine the magnitudes of the principal values of the  $g$ -tensor from a powder spectrum [136, 205]. For example, if there is cylindrical symmetry and no hyperfine splitting the spectrum may just comprise two features from which  $g_{\parallel}$  and  $g_{\perp}$  can be obtained directly. The point is that there can be no absorption at higher or lower fields than the principal values of the  $g$ -tensor and the onset of absorption gives rise to quite sharp features in the derivative curve, even though the intervening absorption is weak. The way in which the lineshape arises can be understood by reference to Fig. 6.1, which shows sketches of the idealised absorption curve, the absorption modified to allow for the finite linewidth and the derivative, for cases of axial and orthorhombic symmetry. When there is hyperfine splitting it may be resolved on one or more of the  $g$ -features. This is illustrated in the spectrum of vanadyl acetyl acetonate in Fig. 6.2. In this

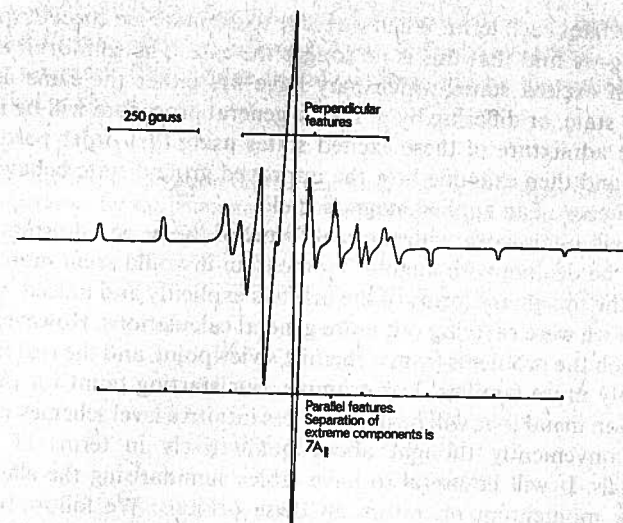


FIG. 6.2. Spectrum of vanadyl acetyl acetonate in a rigid glass.

sort of system, where there is no doubt that the principal axes of the  $g$ - and hyperfine-tensors are parallel, the elements of both tensors can be determined from the powder spectrum. Many transition metal complexes and inorganic radicals have sufficient  $g$ -anisotropy for their powder spectra to be analysed in this way. Where there is more than one hyperfine splitting resolved, or where the anisotropy is smaller, computer simulation of the spectra may give quite precise values of the anisotropic parameters [206].

### 6.3 Some Useful Matrix Elements

Before we set out to calculate  $g$ -tensors it will be helpful to recognise the general methods employed and to tabulate some useful matrix elements. The problem is essentially this. We are concerned with atoms and ions which are under the electrostatic influence of their neighbours so that orbital degeneracy, for instance that characteristic of the five  $d$ -orbitals in a free transition metal ion, is partially or wholly lifted. As explained in Chapter 2, complete lifting of the orbital degeneracy results in the complete quenching of the orbital angular momentum so the magnetic moment should correspond to the spin-only value. The ground state should then consist of functions which are 'pure' with respect to the spin, i.e. even a wavefunction which includes contributions to the spatial part from excited configurations should have the same spin factor ( $\alpha$  or  $\beta$  for

a doublet) for each term. When we come to examine the effect of spin-orbit coupling we find that this is no longer the case. The spin-orbit coupling mixes in excited states which may have  $M_s$  either the same as in the ground state, or differing by  $\pm 1$ . Our general procedure will be to calculate the admixture of these excited states using first order perturbation theory and then examine how the improved ground state behaves under the influence of an applied magnetic field.

We will often work with the real forms of the  $p$ - and  $d$ -orbitals. Since we will be dealing with angular momentum it would seem more natural to use the imaginary forms of the orbitals explicitly and indeed we would do so if we were carrying out more general calculations. However we will approach the problems from a chemist's viewpoint, and the real forms are probably more familiar. For example, our starting point for discussing transition metal ions will be more or less intuitive level schemes which are most conveniently thought about qualitatively in terms of the real  $d$ -orbitals. It will be useful to have tables summarising the effect of the angular momentum operators on these orbitals. We follow the phase conventions of Condon and Shortley [207] so that in terms of the eigenfunctions of the orbital angular momentum operators  $l^2, l_z$ , which we write as  $|l, m\rangle$ , the real orbitals are:

$$p_x = -(1/\sqrt{2})\{|1, +1\rangle - |1, -1\rangle\}$$

$$p_y = (i/\sqrt{2})\{|1, +1\rangle + |1, -1\rangle\} \quad (6.10)$$

$$p_z = |1, 0\rangle$$

$$d_{x^2-y^2} = (1/\sqrt{2})\{|2, 2\rangle + |2, -2\rangle\}$$

$$d_{xy} = -(i/\sqrt{2})\{|2, 2\rangle - |2, -2\rangle\}$$

$$d_{xz} = -(1/\sqrt{2})\{|2, 1\rangle - |2, -1\rangle\} \quad (6.11)$$

$$d_{yz} = (i/\sqrt{2})\{|2, 1\rangle + |2, -1\rangle\}$$

$$d_{z^2} = |2, 0\rangle$$

The modes of operation of  $l_x, l_y$  and  $l_z$  on these orbitals are summarised in Table 6.1. The way to use this table is that the operator at the top of a column operating on the function at the left of a row produces the result entered in the table at the intersection of the row and column. For convenient reference Table 6.2 gives a similar tabulation for the spin operators in the case  $S = \frac{1}{2}$ : it is simply a summary of equations (1.7) and (1.9). Using Tables 6.1 and 6.2 it is easy to construct the matrices of the Zeeman

and spin-orbit coupling Hamiltonians, for one electron, in bases of the real  $p$ - and  $d$ -orbitals. Tables 6.3 and 6.4 give the matrices of the spin-orbit coupling operator. Their value in calculations will be illustrated in the next section.

TABLE 6.1. Modes of operation on the real forms of the  $p$ - and  $d$ -orbitals of the operators for the components of the orbital angular momentum

	$l_x$	$l_y$	$l_z$
$ p_x\rangle \equiv  x\rangle$	0	$-i z\rangle$	$i y\rangle$
$ p_y\rangle \equiv  y\rangle$	$i z\rangle$	0	$-i x\rangle$
$ p_z\rangle \equiv  z\rangle$	$-i y\rangle$	$i x\rangle$	0
$ d_{x^2-y^2}\rangle \equiv  x^2 - y^2\rangle$	$-i yz\rangle$	$-i xz\rangle$	$2i xy\rangle$
$ d_{xy}\rangle \equiv  xy\rangle$	$i xz\rangle$	$-i yz\rangle$	$-2i x^2 - y^2\rangle$
$ d_{yz}\rangle \equiv  yz\rangle$	$i x^2 - y^2\rangle + i\sqrt{3} z^2\rangle$	$i xy\rangle$	$-i xz\rangle$
$ d_{xz}\rangle \equiv  xz\rangle$	$-i xy\rangle$	$i x^2 - y^2\rangle - i\sqrt{3} z^2\rangle$	$i yz\rangle$
$ d_{z^2}\rangle \equiv  z^2\rangle$	$-i\sqrt{3} yz\rangle$	$i\sqrt{3} xz\rangle$	0

TABLE 6.2. Modes of operation of the components of the spin operator for  $S = \frac{1}{2}$

	$S_x$	$S_y$	$S_z$
$ \alpha\rangle$	$+\frac{1}{2} \beta\rangle$	$\frac{1}{2}i \beta\rangle$	$\frac{1}{2} \alpha\rangle$
$ \beta\rangle$	$+\frac{1}{2} \alpha\rangle$	$-\frac{1}{2}i \alpha\rangle$	$-\frac{1}{2} \beta\rangle$

TABLE 6.3. Matrix of  $l$ .s in the basis of real  $p$ -orbitals

	$ x, \alpha\rangle$	$ y, \alpha\rangle$	$ z, \alpha\rangle$	$ x, \beta\rangle$	$ y, \beta\rangle$	$ z, \beta\rangle$
$\langle x, \alpha $	0	$-i/2$	0	0	0	$+1/2$
$\langle y, \alpha $	$i/2$	0	0	0	0	$-i/2$
$\langle z, \alpha $	0	0	0	0	$i/2$	0
$\langle x, \beta $	0	0	$-1/2$	0	$i/2$	0
$\langle y, \beta $	0	0	$-i/2$	$-i/2$	0	0
$\langle z, \beta $	$1/2$	$i/2$	0	0	0	0



TABLE 6.4. Matrix of  $\mathbf{l} \cdot \mathbf{s}$  in the basis of real  $d$ -orbitals

	$ x^2 - y^2, \alpha\rangle$	$ xy, \alpha\rangle$	$ yz, \alpha\rangle$	$ xz, \alpha\rangle$	$ z^2, \alpha\rangle$	$ x^2 - y^2, \beta\rangle$	$ xy, \beta\rangle$	$ yz, \beta\rangle$	$ xz, \beta\rangle$	$ z^2, \beta\rangle$
$\langle x^2 - y^2, \alpha  $	0	-i	0	0	0	0	0	+i/2	+1/2	0
$\langle xy, \alpha  $	+i	0	0	0	0	0	0	0	-i/2	0
$\langle yz, \alpha  $	0	0	0	i/2	0	-i/2	-1/2	0	0	-i/2
$\langle xz, \alpha  $	0	0	-i/2	0	0	-1/2	+i/2	0	0	0
$\langle z^2, \alpha  $	0	0	0	0	0	0	0	+i/2	0	0
$\langle x^2 - y^2, \beta  $	0	0	+i/2	-1/2	0	0	+i	0	0	0
$\langle xy, \beta  $	0	0	-1/2	i/2	0	-i	0	0	0	0
$\langle yz, \beta  $	-i/2	+i/2	0	0	0	0	0	0	-i/2	0
$\langle xz, \beta  $	+1/2	+i/2	0	0	0	0	0	0	0	0
$\langle z^2, \beta  $	0	0	+i/2	+1/2	0	0	0	+i/2	0	0

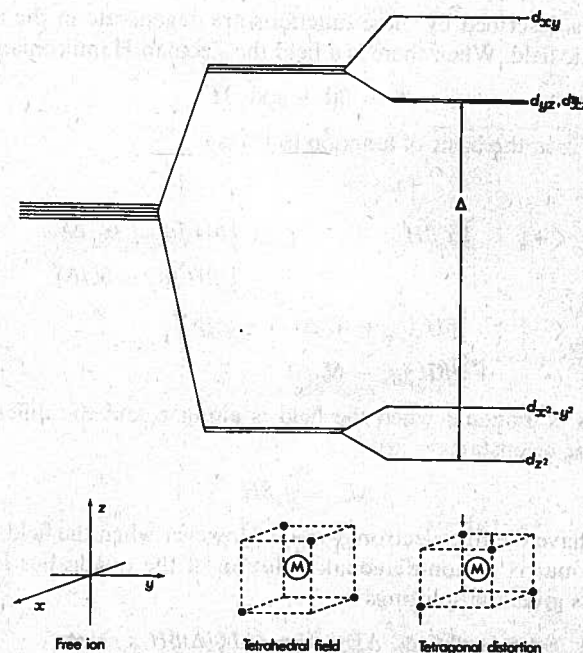
X

6.4  $g$ -Tensors of Some  $S = \frac{1}{2}$  Transition Metal Systems

In order to understand how the programme outlined in the previous section works out in practice we will carry out calculations of the  $g$ -tensors for three models of transition metal systems. We consider  $d^1$ ,  $d^5$  and  $d^9$  cases which, for example, could be taken to represent  $\text{Ti}^{3+}$ ,  $\text{Mn}^{2+}$  or  $\text{Fe}^{3+}$  (low spin) and  $\text{Cu}^{2+}$  respectively.

(i)  $d^1$  System. We consider a  $d^1$  ion in a tetragonally distorted tetrahedral environment. The splitting of the  $d$ -orbitals is illustrated in Fig. 6.3: the tetragonal distortion lifts the spatial degeneracy of  $d_{xz}$  and  $d_{x^2-y^2}$  in the tetrahedral field, and  $d_{xz}$  is the singly occupied orbital. If there were no spin-orbit coupling the ground state wavefunctions would just be  $|d_{xz}, \alpha\rangle$  and  $|d_{xz}, \beta\rangle$ . We have to find new wavefunctions in which small amounts of excited states are mixed with these.

From Table 6.4 we can see that the spin-orbit coupling mixes  $|d_{xz}, \alpha\rangle$  with  $|d_{yz}, \alpha\rangle$  and  $|d_{xz}, \beta\rangle$ . First-order perturbation theory gives the admixture

FIG. 6.3. Level scheme for the  $d$ -orbitals in a trigonally distorted tetrahedral crystal field.

coefficient of excited state  $|i\rangle$ , energy  $E_i$ , with ground state  $|0\rangle$ , energy  $E_0$ , due to the perturbation  $\mathcal{H}'$  as

$$C_{0,i} = - \frac{\langle i | \mathcal{H}' | 0 \rangle}{E_i - E_0} \quad (6.12)$$

We have

$$\mathcal{H}' = \zeta \mathbf{l} \cdot \mathbf{s} \quad (6.13)$$

so (6.12) can be written

$$C_{0,i} = - (\zeta/\Delta) \langle i | \mathbf{l} \cdot \mathbf{s} | 0 \rangle \quad (6.14)$$

The energy difference  $\Delta$  for our particular problem is indicated in Fig. 6.3. Using (6.14) and Table 6.4 we can write down straight away the first-order improved ground state wavefunctions. They are

$$\begin{aligned} |+\rangle &= |d_{z^2}, \alpha\rangle + (\sqrt{3}/2)i(\zeta/\Delta)|d_{yz}, \beta\rangle + (\sqrt{3}/2)(\zeta/\Delta)|d_{xz}, \beta\rangle \\ |-\rangle &= |d_{z^2}, \beta\rangle + (\sqrt{3}/2)i(\zeta/\Delta)|d_{yz}, \alpha\rangle - (\sqrt{3}/2)(\zeta/\Delta)|d_{xz}, \alpha\rangle \end{aligned} \quad (6.15)$$

The states described by these functions are degenerate in the absence of a magnetic field. When there is a field the Zeeman Hamiltonian is

$$\mathcal{H} = \beta(\mathbf{l} + g_e \mathbf{s}) \cdot \mathbf{H} \quad (6.16)$$

whose matrix in the basis of function (6.15) is

$$\begin{array}{cc} & \begin{array}{c} |+\rangle \\ |-\rangle \end{array} \\ \begin{array}{c} \langle +| \\ \langle -| \end{array} & \begin{array}{cc} \frac{1}{2}g_e\beta H_z & \frac{1}{2}\beta H_x(g_e - 6\zeta/\Delta) \\ & -\frac{1}{2}\beta H_y(g_e - 6\zeta/\Delta) \\ \frac{1}{2}\beta H_x(g_e - 6\zeta/\Delta) & -\frac{1}{2}g_e\beta H_z \\ +\frac{1}{2}i\beta H_y(g_e - 6\zeta/\Delta) & \end{array} \end{array} \quad (6.17)$$

This matrix is diagonal when the field is along  $z$ , and the difference in energy of the eigenstates is just

$$\Delta E_z = g_e \beta H \quad (6.18)$$

so that we have the free electron  $g$ -value. However when the field is along  $x$  or  $y$  the matrix is non-diagonal. Solution of the quadratics for these orientations gives the splittings

$$\Delta E_x = \Delta E_y = (g_e - 6\zeta/\Delta)\beta H \quad (6.19)$$

and we see that, since both  $\zeta$  and  $\Delta$  are positive, the  $g$ -values are less than the free-electron value. We observe that the symmetry of the crystal field

determines the axial symmetry of the  $g$ -tensor and of course, the directions of its principal values. We can summarise the results as

$$g_{\parallel} = g_e; \quad g_{\perp} = (g_e - 6\zeta/\Delta) \quad (6.20)$$

(ii) *Low spin  $d^5$  system.* A simplifying feature of the calculation we have just carried out was that we only had one electron to worry about. We now see what happens when the metal ion has several electrons, so that its states have to be described by determinantal functions. To illustrate the method we will use a simplified version of the calculation carried out by Fortman and Hayes for the  $\{\text{Mn}(\text{CN})_5\text{NO}\}^{2-}$  ion [208]. The original paper was concerned with covalent bonding, but we will adopt a crystal field approach.

Our starting point is the level scheme shown at the right hand side of Fig. 6.4, corresponding to a tetragonally distorted octahedral field.

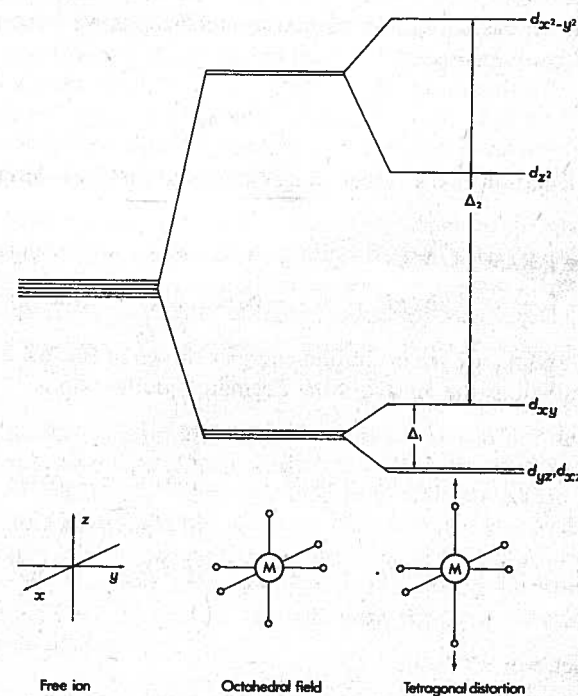


FIG. 6.4. Level scheme for the  $d$ -orbitals in a tetragonally distorted octahedral crystal field.



Feeding in the five electrons, we have that  $d_{xy}$  is the singly occupied orbital. We write the zero-order wavefunctions for  $\alpha$  and  $\beta$  spin as

$$\begin{aligned} |xy\rangle &= |(xz)(\bar{xz})(yz)(\bar{yz})(xy)| \\ |\bar{xy}\rangle &= |(xz)(\bar{xz})(yz)(\bar{yz})(\bar{xy})| \end{aligned} \quad (6.21)$$

thus defining a new contracted notation. From Table 6.4 we see that excited states which can obviously be mixed with these are those in which an electron is promoted from  $(xz)$  or  $(yz)$  to  $(xy)$  and those in which the unpaired electron is promoted to  $(x^2 - y^2)$ . There are other possibilities which we will consider later, but these will do for a start. We will write the wavefunctions for these excited states as

$$\begin{aligned} |xz\rangle &= |(xz)(yz)(\bar{yz})(xy)(\bar{xy})| \\ |x^2 - y^2\rangle &= |(xz)(\bar{xz})(yz)(\bar{yz})(x^2 - y^2)| \end{aligned} \quad (6.22)$$

and so on. In evaluating the admixture coefficients we have to use the spin-orbit coupling operator

$$\mathcal{H}' = \sum_{i=1}^5 \zeta_i \cdot \mathbf{s}_i \quad (6.23)$$

so the calculation takes rather longer than the first one. Eventually we obtain

$$\begin{aligned} |+\rangle &= |xy\rangle + (i\zeta/\Delta_2)|x^2 - y^2\rangle + (i\zeta/2\Delta_1)|\bar{xz}\rangle + (\zeta/2\Delta_1)|\bar{yz}\rangle \\ |-\rangle &= |\bar{xy}\rangle - (i\zeta/\Delta_2)|x^2 - y^2\rangle + (i\zeta/2\Delta_1)|xz\rangle - (\zeta/2\Delta_1)|yz\rangle \end{aligned} \quad (6.24)$$

where  $\Delta_1$  and  $\Delta_2$  are the excitation energies shown in Fig. 6.4. In the basis of these functions the matrix of the Zeeman Hamiltonian is

$$\begin{array}{cc} & \begin{array}{c} |+\rangle \\ |-\rangle \end{array} \\ \begin{array}{c} \langle +| \\ \langle -| \end{array} & \begin{array}{cc} \frac{1}{2}\beta H_z(g_e - 8\zeta/\Delta_2) & \frac{1}{2}\beta H_x(g_e + 2\zeta/\Delta_1) \\ & -\frac{1}{2}i\beta H_y(g_e + 2\zeta/\Delta_1) \\ \frac{1}{2}\beta H_x(g_e + 2\zeta/\Delta_1) & -\frac{1}{2}\beta H_z(g_e - 8\zeta/\Delta_2) \\ +\frac{1}{2}i\beta H_y(g_e + 2\zeta/\Delta_1) & \end{array} \end{array} \quad (6.25)$$

from which we can see that

$$\begin{aligned} g_z = g_{||} &= (g_e - 8\zeta/\Delta_2) \\ g_x = g_y = g_{\perp} &= (g_e + 2\zeta/\Delta_1) \end{aligned} \quad (6.26)$$

These values illustrate an important general result: admixture of excited states in which an electron is promoted from a filled orbital to the half-filled orbital leads to an increase in the  $g$ -factor from the free electron value, while the  $g$ -factor is decreased if the excited state is formed by promotion of the unpaired electron to a vacant orbital. This principle is quite useful for making a qualitative estimate of the level scheme in a new complex. For  $\{\text{Mn}(\text{CN})_5\text{NO}\}^{2-}$  Fortman and Hayes [208] measured  $g_{||} = 1.9892$ ,  $g_{\perp} = 2.0265$ : these values are smaller and larger than the free spin value, but in view of our crystal field type of treatment we should not seriously try to explain them just using (6.26).

Apart from the neglect of covalent bonding our treatment is also incomplete in that we have not taken account of all the possible excited states. There are four more configurations which we should consider, formed by promoting an electron from  $(xz)$  or  $(yz)$  to  $(z^2)$  or  $(x^2 - y^2)$ . These configurations have three singly occupied orbitals and we have to form suitable linear combinations to obtain eigenfunctions of  $S^2, S_z$  (cf. Section 3.4). Thus their inclusion makes the calculation longer, though there is nothing really different from what we have done already. Fortman and Hayes [208] included them in their calculation and showed that in fact their respective contributions to the  $g$ -tensor (to  $g_{||}$ ) could reasonably be expected to cancel one another out. That particular conclusion does not necessarily mean that one would always be justified in neglecting this type of excited state.

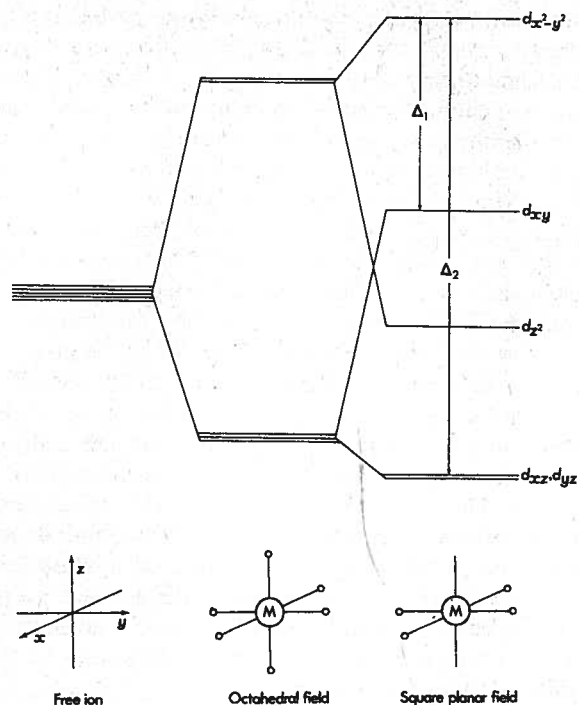
(iii)  $d^9$  System. Complexes of  $\text{Cu}^{2+}$  are very amenable to study by e.s.r. and it is probably the most-studied transition metal ion, so it is appropriate that we should include a calculation on a model system for this ion. We choose a square planar array of ligands, since this is common for  $\text{Cu}^{2+}$ .

The usual crystal field argument, for an extreme tetragonal distortion of an octahedron, indicates the level scheme shown in Fig. 6.5, so the singly occupied orbital should be  $d_{x^2-y^2}$ , the orbital pointing directly at the ligands. The ground and excited states of the ion are described by determinantal functions of the coordinates of nine electrons so it looks as though the evaluation of matrix elements of one-electron operators between these would be even lengthier than in our previous calculation. With practice, it is not too bad, but it turns out that we can save even that labour, for the problem can be handled just like a one-electron problem. We are able to do this because the spin-orbit coupling Hamiltonian can be written in the form

$$\mathcal{H}' = \lambda \mathbf{L} \cdot \mathbf{S} \quad (6.27)$$

where

$$\lambda = \pm \zeta/2S \quad (6.28)$$

FIG. 6.5. Level scheme for the  $d$ -orbitals in a square planar crystal field.

with the positive sign if the shell is less than half full (up to four  $d$ -electrons) and the negative sign if the shell is more than half full. This important general result is discussed in detail by Condon and Shortley [207] and by Griffith [8] and we will not derive it here. Qualitatively, it follows from the fact that the matrix elements of  $\sum \mathbf{l}_i \cdot \mathbf{s}_i$  within a term can be expressed as a product of elements of  $\mathbf{l}_i$  and of  $\mathbf{s}_i$  separately. In treating  $\text{Cu}^{2+}$  using (6.27) one is effectively doing the calculation for a positive hole rather than for the nine electrons. The language of 'positive holes' or 'positrons' is commonly used in discussions of shells which are more than half full.

The calculation of the  $g$ -tensor is straightforward, following the lines of the previous examples. We find that the first order wavefunctions are

$$\begin{aligned} |+\rangle &= |x^2 - y^2\rangle + (i\lambda/\Delta_1)|xy\rangle - (i\lambda/2\Delta_2)|\bar{y}z\rangle + (\lambda/2\Delta_2)|\bar{x}z\rangle \\ |-\rangle &= |x^2 - y^2\rangle - (i\lambda/\Delta_1)|\bar{x}y\rangle - (i\lambda/2\Delta_2)|yz\rangle - (\lambda/2\Delta_2)|xz\rangle \end{aligned} \quad (6.29)$$

where the energy differences are defined in Fig. 6.5. These functions lead to the  $g$ -values,

$$\begin{aligned} g_z &= g_{\parallel} = g_e + 8\lambda/\Delta_1 \\ g_x &= g_y = g_{\perp} = g_e + 2\lambda/\Delta_2 \end{aligned} \quad (6.30)$$

As we expect, these values are greater than the free-spin value since all the excited states of interest must arise by promotion of an electron into the orbital which is singly occupied in the zero-order ground state. When allowance is made for covalent bonding the results (6.30) are in good accord with the experimental results for square planar copper complexes.

### 6.5 General Theory for Transition Metal Ions

Having developed a general quantitative understanding of the nature of the  $g$ -tensor in the previous section we will go on now to present a more general theory. The derivation is fairly lengthy but we will go through the argument in detail as it is a cornerstone of e.s.r. theory. The result was originally derived by Pryce [209], and his paper was fundamental to the whole development of the concept of the spin Hamiltonian. Our presentation parallels that given by Slichter [14]. Before starting we should note that the perturbation theory technique we use is of much more general applicability, being particularly appropriate for handling cases in which there is degeneracy.

We consider a metal ion in a crystal, and write the Hamiltonian as a sum of three terms,

$$\mathcal{H} = \mathcal{H}_0 + \mathcal{H}_1 + \mathcal{H}_2 \quad (6.31)$$

$\mathcal{H}_0$  is the principal electronic part: it includes the usual intra-atomic terms and the effect of the crystal field.  $\mathcal{H}_1$  and  $\mathcal{H}_2$  are going to be taken as perturbations. They are

$$\mathcal{H}_1 = g_e \beta \mathbf{H} \cdot \mathbf{S} \quad (6.32)$$

and

$$\mathcal{H}_2 = \beta \mathbf{H} \cdot \mathbf{L} + \lambda \mathbf{L} \cdot \mathbf{S} \quad (6.33)$$

We note again that the theory will not be appropriate for rare-earth ions, for which the crystal field splitting will not be larger than the spin-orbit coupling. The eigenfunctions of  $\mathcal{H}_0$  can be written as simple products of an orbital factor, which we will label with  $n$ , and a spin factor, labelled with  $s$ ,

$$\mathcal{H}_0 |n, s\rangle = E_n |n, s\rangle \quad \checkmark \quad (6.34)$$



Now, in the  $|n, s\rangle$  basis the only non-zero matrix elements of  $\mathcal{H}_1$  are diagonal in  $n$ , while, since the orbital angular momentum is assumed to be quenched,  $\mathcal{H}_2$  has only matrix elements which are off-diagonal in  $n$ . If we only had one of the perturbations the matrix of the Hamiltonian would be block-diagonal and the problem of finding the eigenvalues would be simplified. The presence of  $\mathcal{H}_1$  and  $\mathcal{H}_2$  together means that in general the matrix has no such simplifying feature.

We can think of approaching the problem in two ways. Either, we could seek a new basis to make the matrix block-diagonal, or we could seek to transform the Hamiltonian to reduce to zero the matrix elements between states of different  $n$ . These processes are equivalent, as we can see by considering the first. If we denote the new basis with Greek letters we can write

$$|\eta, \sigma\rangle = \exp(iT)|n, s\rangle \quad (6.35)$$

where  $T$  is some Hermitian operator. We also have

$$\langle\eta, \sigma| = \langle n, s| \exp(-iT), \quad (6.36)$$

and the matrix elements of the Hamiltonian in the new basis are

$$\begin{aligned} \langle\eta, \sigma|\mathcal{H}|\eta, \sigma\rangle &= \langle(n, s) \exp(-iT)|\mathcal{H}|\exp(iT)(n, s)\rangle \\ &\equiv \langle n, s| \exp(-iT) \mathcal{H} \exp(iT) |n, s\rangle \end{aligned} \quad (6.37)$$

Thus we may either calculate the matrix elements of the original Hamiltonian in the new basis, or those of a transformed Hamiltonian in the original basis. We will follow the latter course in our calculation. The form of the transformation may appear novel but in fact it is perfectly general. A more familiar procedure would perhaps be to formulate explicitly linear combinations of the complete set of functions  $|n, s\rangle$ ,

$$|\eta, \sigma\rangle = \sum_{n, s} C_{ns} |n, s\rangle \quad (6.38)$$

Comparing the right-hand sides of (6.35) and (6.38) we see that  $\exp(iT)$  is a projection operator which projects out of the single function  $|n, s\rangle$  the linear combination on the right-hand side of (6.38).

We now consider the transformed Hamiltonian,  $\mathcal{H}'$ , in more detail,

$$\mathcal{H}' = \exp(-iT) \mathcal{H} \exp(iT) \quad (6.39)$$

Since the matrix elements originally off-diagonal in  $n$  were small, we can take  $T$  to be small, so we develop (6.39) by expanding the exponentials to second order,

$$\begin{aligned} \mathcal{H}' &= (1 - iT - T^2/2) \mathcal{H} (1 + iT - T^2/2) \\ &= \mathcal{H} + i[\mathcal{H}, T] - \frac{1}{2}[[\mathcal{H}, T], T] \\ &= \mathcal{H}_0 + \mathcal{H}_1 + \mathcal{H}_2 + i[\mathcal{H}_0 + \mathcal{H}_1, T] + i[\mathcal{H}_2, T] \\ &\quad - \frac{1}{2}[[\mathcal{H}_0 + \mathcal{H}_1, T], T] - \frac{1}{2}[[\mathcal{H}_2, T], T] \end{aligned} \quad (6.40)$$

We now choose

$$\mathcal{H}_2 + i[\mathcal{H}_0 + \mathcal{H}_1, T] = 0 \quad (6.41)$$

so that the third and fourth terms of (6.40) drop out, while the sixth term becomes

$$-\frac{1}{2}[[\mathcal{H}_0 + \mathcal{H}_1, T], T] = -\frac{1}{2}[i\mathcal{H}_2, T] = -(i/2)[\mathcal{H}_2, T] \quad (6.42)$$

Furthermore, the last term on the right of (6.40) is essentially third order so we drop it. After these steps (6.40) has become

$$\mathcal{H}' = \mathcal{H}_0 + \mathcal{H}_1 + (i/2)[\mathcal{H}_2, T] \quad (6.43)$$

Before we can use this Hamiltonian we need to know something about the matrix elements of  $T$ , for which operator we still have no explicit form. We calculate a matrix element of (6.41),

$$\langle n's'|\mathcal{H}_2 + i[\mathcal{H}_0 + \mathcal{H}_1, T]|ns\rangle = 0 \quad (6.44)$$

Expanding the commutator and matrix elements of products of operators this becomes

$$\begin{aligned} \langle n's'|\mathcal{H}_2|ns\rangle + i \sum_{n''s''} \{ \langle n's'|\mathcal{H}_0|n''s''\rangle \langle n''s''|T|ns\rangle \\ - \langle n's'|T|n''s''\rangle \langle n''s''|\mathcal{H}_0|ns\rangle \} \\ + i \sum_{n''s''} \{ \langle n's'|\mathcal{H}_1|n''s''\rangle \langle n''s''|T|ns\rangle \\ - \langle n's'|T|n''s''\rangle \langle n''s''|\mathcal{H}_1|ns\rangle \} = 0 \end{aligned} \quad (6.45)$$

$\mathcal{H}_0$  is diagonal in  $|ns\rangle$  so in the first term in  $\mathcal{H}_0$  we must have  $n''s'' = n's'$ , while in the second,  $n''s'' = ns$ .  $\mathcal{H}_1$  has no matrix elements off-diagonal in  $n$  so in the first term in  $\mathcal{H}_1$  we must have  $n'' = n'$ , and in the second,  $n'' = n$ . With these conditions, and using (6.34), (6.45) reduces to

$$\begin{aligned} \langle n's'|\mathcal{H}_2|ns\rangle + i(E_{n'} - E_n) \langle n's'|T|ns\rangle \\ + i \sum_{s''} \{ \langle n's'|\mathcal{H}_1|n's''\rangle \langle n's''|T|ns\rangle - \langle n's'|T|ns''\rangle \langle ns''|\mathcal{H}_1|ns\rangle \} = 0 \end{aligned} \quad (6.46)$$

There are now two cases to consider. First, if  $n \neq n'$ . The terms under the summation, being a difference of products of small matrix elements, can be neglected compared to the second term. Thus we obtain

$$\langle n's'|T|ns\rangle = \frac{\langle n's'|\mathcal{H}_2|ns\rangle}{i(E_n - E_{n'})}; \quad (n \neq n') \quad (6.47)$$

Second, if  $n = n'$ , (6.46) becomes

$$\sum_{s''} \langle ns'|\mathcal{H}_1|ns''\rangle \langle ns''|T|ns\rangle = \sum_{s''} \langle ns'|T|ns''\rangle \langle ns''|\mathcal{H}_1|ns\rangle \quad (6.48)$$

which is certainly true if

$$\langle ns''|T|ns\rangle = 0 \quad (6.49)$$

Equations (6.47) and (6.49) now enable us to calculate the matrix elements of the transformed Hamiltonian (6.43).

We consider first the elements which are off-diagonal in  $n$ . Since  $\mathcal{H}_0$  and  $\mathcal{H}_1$  are diagonal in  $n$  we have

$$\langle n's'|\mathcal{H}'|ns\rangle = (i/2)\langle n's'|[\mathcal{H}_2, T]|ns\rangle \quad (6.50)$$

Expanding the commutator and using (6.47) we obtain

$$\langle n's'|\mathcal{H}'|ns\rangle = \frac{1}{2} \sum_{n''s''} \langle n's'|\mathcal{H}_2|n''s''\rangle \langle n''s''|\mathcal{H}_2|ns\rangle \left\{ \frac{1}{E_n - E_{n''}} - \frac{1}{E_{n''} - E_{n'}} \right\} \quad (6.51)$$

So we see that the off-diagonal matrix elements of the new Hamiltonian are reduced, by a factor of the reciprocal of the energy difference between eigenstates of  $\mathcal{H}_0$ , compared to those of  $\mathcal{H}_2$ . Since the energy differences involved are large the off-diagonal matrix elements of  $\mathcal{H}'$  must be small, and so they can be neglected. To calculate the matrix elements of  $\mathcal{H}'$  which are diagonal in  $n$  we have to consider

$$\langle ns'|\mathcal{H}'|ns\rangle = \langle ns'|\mathcal{H}_0|ns\rangle + \langle ns'|\mathcal{H}_1|ns\rangle + (i/2)\langle ns'|[\mathcal{H}_2, T]|ns\rangle \quad (6.52)$$

The first term gives

$$\langle ns'|\mathcal{H}_0|ns\rangle = E_n \delta_{s's} \quad (6.53)$$

and the second term is also straightforward. For the third term we obtain

$$(i/2)\langle ns'|[\mathcal{H}_2, T]|ns\rangle = \sum_{n's''} \frac{\langle ns'|\mathcal{H}_2|n's''\rangle \langle n's''|\mathcal{H}_2|ns\rangle}{E_n - E_{n'}} \quad (6.54)$$

Collecting the contributions to the matrix element we have,

$$\langle ns'|\mathcal{H}'|ns\rangle = E_n \delta_{s's} + \langle ns'|\mathcal{H}_1|ns\rangle + \sum_{n's''} \frac{\langle ns'|\mathcal{H}_2|n's''\rangle \langle n's''|\mathcal{H}_2|ns\rangle}{E_n - E_{n'}} \quad (6.55)$$

We have now obtained our general result. Let us see what it is. The original matrix was awkward because it had elements off-diagonal in both  $n$  and  $s$ . The discussion shows that we can get a good approximation to the eigenvalues by diagonalising a matrix which is diagonal in  $n$ . This is still the matrix of  $\mathcal{H}_0$  and  $\mathcal{H}_1$ , but instead of  $\mathcal{H}_2$  we have the operator whose matrix elements are defined by the third term on the right of (6.55). We now develop (6.55) using the explicit forms of the operators.

Straightforward calculation gives, for a typical matrix element of the Hamiltonian,

$$\begin{aligned} \langle ns'|\mathcal{H}'|ns\rangle &= \langle ns'|\mathcal{H}_0|ns\rangle + \sum_{\mu=x,y,z} \langle ns'|g_e \beta H_\mu S_\mu|ns\rangle \\ &+ \sum_{n''s''} \sum_{\mu, \nu=x,y,z} \{ \langle ns'|\beta H_\mu L_\mu|n''s''\rangle \langle n''s''|\beta H_\nu L_\nu|ns\rangle / E_n - E_{n''} \\ &+ \langle ns'|\beta H_\mu L_\mu|n''s''\rangle \langle n''s''|\lambda L_\nu S_\nu|ns\rangle / E_n - E_{n''} \\ &+ \langle ns'|\lambda L_\mu S_\mu|n''s''\rangle \langle n''s''|\beta H_\nu L_\nu|ns\rangle / E_n - E_{n''} \\ &+ \langle ns'|\lambda L_\mu S_\mu|n''s''\rangle \langle n''s''|\lambda L_\nu S_\nu|ns\rangle / E_n - E_{n''} \} \end{aligned} \quad (6.56)$$

The first term gives the absolute energy of state  $|n\rangle$  in the absence of spin-orbit and Zeeman interactions. If we subtract this term we simply redefine the energy zero, and we can now carry out the integration over the spatial coordinates. It is convenient to define

$$\Lambda_{\mu\nu} = \sum_{n''s''} \sum_{\mu, \nu=x,y,z} \frac{\langle ns'|L_\mu|n''s''\rangle \langle n''s''|L_\nu|ns\rangle}{E_n - E_{n''}} \quad (6.57)$$

in calculating the matrix elements of  $\mathcal{H}''$ ,

$$\mathcal{H}'' = \mathcal{H}' - \mathcal{H}_0 \quad (\equiv \mathcal{H}_1 + \mathcal{H}_2) \quad (6.58)$$

We obtain

$$\begin{aligned} \langle s'|\mathcal{H}''|s\rangle &= \sum_{\mu=x,y,z} \langle s'|g_e \beta H_\mu S_\mu|s\rangle + \sum_{\mu, \nu=x,y,z} \{ \Lambda_{\mu\nu} H_\mu H_\nu \langle s'|s\rangle \\ &+ \lambda \beta H_\mu \Lambda_{\mu\nu} \langle s'|S_\nu|s\rangle + \lambda \beta H_\nu \Lambda_{\mu\nu} \langle s'|S_\mu|s\rangle + \lambda^2 \Lambda_{\mu\nu} \langle s'|S_\mu S_\nu|s\rangle \} \end{aligned} \quad (6.59)$$



where we have kept the order of the terms as in (6.56). This result shows that we can describe the energy of the system in a magnetic field with an effective Hamiltonian

$$\mathcal{H} = \sum_{\mu, \nu=x, y, z} \{g_{\mu} \beta H_{\mu} S_{\mu} + 2\lambda \beta \Lambda_{\mu\nu} H_{\mu} S_{\nu} + \lambda^2 \Lambda_{\mu\nu} S_{\mu} S_{\nu} + \beta^2 \Lambda_{\mu\nu} H_{\mu} H_{\nu}\} \quad (6.60)$$

We can also write the result as

$$\mathcal{H} = \sum_{\mu, \nu=x, y, z} \{\beta(g_{\mu} \delta_{\mu\nu} + 2\lambda \Lambda_{\mu\nu}) H_{\mu} S_{\nu} + \lambda^2 \Lambda_{\mu\nu} S_{\mu} S_{\nu} + \beta^2 \Lambda_{\mu\nu} H_{\mu} H_{\nu}\} \quad (6.61)$$

Equations (6.60) and (6.61) express the general form of the effective spin Hamiltonian as derived by Pryce [209]. The first term in (6.61) gives the general form of the  $g$ -tensor, and we will return to it later. The second term is a second-order contribution from the spin-orbit coupling: it is equivalent to a tensorial spin-spin coupling and its effect is analogous to that of the dipolar spin-spin coupling discussed in the previous chapter. The final term is spin-independent and we will be able to drop it in discussing e.s.r. spectra: it gives a temperature-independent contribution to the paramagnetic susceptibility, however [209].

We conclude this section with a few summarising comments about the  $g$ -tensors of doublet state transition metal ions. In general the position of the resonance is described by the spin Hamiltonian

$$\mathcal{H} = \beta \mathbf{H} \cdot \mathbf{g} \cdot \mathbf{S} \quad (6.62)$$

where the tensor  $\mathbf{g}$  has elements

$$g_{\mu\nu} = g_{\mu} \delta_{\mu\nu} + 2\lambda \Lambda_{\mu\nu} \quad (6.63)$$

and  $\Lambda_{\mu\nu}$  is defined by (6.57). The tensor  $\Lambda_{\mu\nu}$  is symmetric and thus so is  $g_{\mu\nu}$  and both can be simultaneously diagonalised by a suitable choice of axes. In the examples worked out in the previous section we were able to make this choice on symmetry grounds, and this is usually possible. The reader is left to verify for himself that the results derived in the previous section also follow from direct application of (6.63). Finally we note yet again that our results have been derived for a perturbed atom or ion in a strong crystal field: complications occur when there is covalent bonding and delocalisation, while an entirely different approach is necessary if the crystal field is weak compared to the spin-orbit coupling.

## 6.6 Polyatomic Molecules in Doublet States: Inorganic Radicals

It is not a trivial exercise to extend the theory of the previous section to polyatomic species in which the electrons can be delocalised over several centres. The necessary theory has been discussed in detail by Stone [210],

but is too complex for us to reproduce here. We will simply outline qualitatively some of the considerations involved and the approximations made, present the results, and illustrate their use.

It turns out that the orbital contribution to the magnetic moment, as reflected by the  $g$ -tensor, comes essentially as a sum of contributions from angular momentum about each atom. If one takes a doublet species whose ground and excited states are assumed to be adequately described by single spin-orbital configurations in which there is one singly occupied orbital, the principal components of the  $g$ -tensor can be calculated to be [210],

$$g_{\alpha\alpha} = g_e - 2 \sum_n \frac{\sum_{\mu} \langle \psi_0 | \zeta_{\mu} l_{\mu} | \psi_n \rangle \sum_{\nu} \langle \psi_n | l_{\nu} | \psi_0 \rangle}{E_n - E_0} \quad \alpha = x, y, z \quad (6.64)$$

Here  $\psi_0$  is the molecular orbital which is singly occupied in the ground state and the  $\psi_n$  are those which are singly occupied in the excited states.  $E_0$  and  $E_n$  are the orbital energies and  $\zeta_{\mu}$  is the spin-orbit coupling constant for atom  $\mu$ . It is assumed that the molecular orbitals can be expanded in terms of atomic orbitals and overlap neglected, so that when the matrix elements are expanded in terms of the atomic orbitals one only retains terms which are diagonal in  $\mu$ . This amounts to neglecting any orbital angular momentum of an electron in an orbital on one atom about a different nucleus, which is reasonable since the coupling coefficients  $\xi_{\mu}(r_{\mu})$  decrease rapidly with increasing  $r_{\mu}$ . Apart from assumptions about the description of the electronic structures of the ground and excited states there are others. A crucial one in the early stage of the argument is that the Hamiltonian for the spin-orbit coupling can be expressed as a sum of terms for each electron about each atom,

$$\mathcal{H} = \sum_{i, \mu} \xi_{\mu}(r_{i\mu}) \mathbf{l}_{i\mu} \cdot \mathbf{s}_i \quad (6.65)$$

Comparison of (6.64) and (6.63) might suggest that (6.64) is derived by using (6.65) in a treatment analogous to that of the previous section, incorporating molecular rather than atomic orbitals. In fact the justification for (6.64) requires more subtlety. The point is that the general results must be gauge invariant, that is, independent of the choice of origin to which angular momenta are referred. Stone's analysis [210] shows that to obtain results which fulfil this condition it is necessary to include some higher order terms in the full Hamiltonian. The general result shows that there are two contributions to the deviation of the  $g$ -tensor from the free-spin value. However one of these is small and can be neglected and the result (6.64) follows by developing the other, making the assumption about wavefunctions which we have mentioned.

Equation (6.64) contains a result with which we are already familiar. Excited states formed by promoting the unpaired electron into an empty orbital give a negative contribution to the  $g$ -tensor element, reducing it from the free-spin value, because  $E_n > E_0$ . If the excited states are formed by promoting an electron into the half-filled orbital ( $E_n - E_0$ ) is negative and the  $g$ -tensor element is increased above the free-spin value. (cf. Section 6.4). Thus qualitative consideration of the  $g$ -tensor may enable one to decide whether a particular proposed level scheme for the species under consideration is reasonable or not. Further quantitative analysis rapidly becomes harder, in that one soon has more unknowns than experimental information. Even if there is only one excited state to consider one has to know the coefficients in two orbitals and the excitation energy. The latter may be known from the optical spectrum, if it has been assigned, and some of the coefficients in the ground state singly occupied orbital may have been determined from the analysis of the hyperfine splittings, but that still leaves the excited state coefficients unknown. Clearly the difficulties increase as the number of contributing excited states increases. Thus, unless one has the results of a rather good calculation to feed into (6.64) the best one can probably hope for is a semi-quantitative interpretation of relatively large shifts from the free spin value of the  $g$ -tensor elements. In order to illustrate these points and show how (6.64) is used we will outline Ovenall and Whiffen's analysis [138] of the  $g$ -tensor for  $\text{CO}_2^-$ , thus completing the analysis of the spectrum which we started in Section 4.4.

The experimental result [138] is that the principal values of the  $g$ -tensor are

$$g_{xx} = 2.0032, \quad g_{yy} = 1.9975, \quad g_{zz} = 2.0014 \quad (6.66)$$

The  $XX$  and  $ZZ$  elements deviate little from the free spin value and we will not attempt to interpret them: they may be the resultant of near-cancellation of contributions from more than one excited state, or involve predominantly one rather highly excited state. The  $YY$  element deviates much more from the free spin value and we will attempt to interpret it. Assuming that one excited state only is involved, the sign of the  $g$ -shift indicates that we should look for an orbital which is empty in the ground state. Further, the discussion of Section 4.4 indicated that the unpaired electron in the ground state occupied an orbital with appreciable  $p_z$  components so that for angular momentum about the  $y$ -direction the singly occupied orbital in the excited state should have appreciable  $p_x$  character. To proceed further we need to look in somewhat more detail into the expected electronic structure of  $\text{CO}_2^-$ .

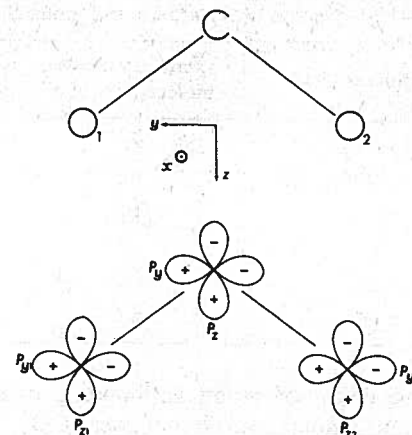


FIG. 6.6. Axes and basis orbitals for  $\text{CO}_2^-$ . The  $p_x$ ,  $p_{x1}$  and  $p_{x2}$ -orbitals, which have their axes perpendicular to the plane of the paper, and the  $2s$ -orbitals,  $s$ ,  $s_1$ ,  $s_2$ , are not shown.

The valence orbitals are the  $2s$ - and  $2p$ -orbitals of carbon and oxygen, and there are 17 valence electrons. The molecule is expected to be bent because, it is isoelectronic with  $\text{NO}_2$ , and, addition of an electron to linear  $\text{CO}_2$  would give an orbitally degenerate species which would be expected to bend to relieve the degeneracy. The basis atomic orbitals and a convenient choice for their phases, are illustrated in Fig. 6.6. The general form of the molecular orbitals must reflect the  $C_{2v}$  symmetry of the radical: the orbitals must be either symmetric (S) or antisymmetric (A) with respect to reflection across the  $xz$ - and  $yz$ -planes, and the atomic orbitals which make up a molecular orbital of given symmetry must behave in the same way under these symmetry operations. The behaviour of the atomic orbitals under the symmetry operations and the symmetry labels for the molecular orbitals are shown in Table 6.5. The Table shows the behaviour of in-phase and out-of-phase combinations of equivalent orbitals on the oxygen atoms since these are what must appear in any molecular orbital to which these atomic orbitals contribute. The total number of molecular orbitals that can be formed is 12 and the number of each symmetry is shown in Table 6.5.

A level scheme which should apply to  $\text{CO}_2^-$  is shown in Fig. 6.7, and according to this the unpaired electron should occupy an orbital of  $a_1$  symmetry, which we can write as

$$\psi_{a1} = c_s s + c_{xc} p_x + c_{xo}(p_{x1} + p_{x2}) + c_{yo}(p_{y1} - p_{y2}) + c_{so}(s_1 + s_2) \quad (6.67)$$



TABLE 6.5. Symmetry classification of the atomic and molecular orbitals of  $\text{CO}_2^-$ 

Symmetry	Atomic orbitals	Symmetry label of molecular orbital	Number of molecular orbitals
$S_{xz}S_{yz}$	$s, p_x, (s_1 + s_2),$ $(p_{y1} - p_{y2}), (p_{x1} + p_{x2})$	$a_1$	5
$S_{xz}A_{yz}$	$p_x, (p_{x1} + p_{x2})$	$b_1$	2
$A_{xz}S_{yz}$	$p_y, (s_1 - s_2), (p_{y1} + p_{y2})$ $(p_{z1} - p_{z2})$	$b_2$	4
$A_{xz}A_{yz}$	$(p_{x1} - p_{x2})$	$a_2$	1

This orbital can be described as an antibonding pseudo- $\pi$ -orbital: it correlates with an antibonding  $\pi$ -orbital of linear  $\text{CO}_2$ . Thus  $c_{xc}$  and  $c_{xo}$  are expected to have opposite signs. Further, the coefficients  $c_{yo}$  and  $c_{so}$  are expected to be small, and we will find that our analysis confirms this. We have already estimated  $c_{sc}$  and  $c_{xc}$  from analysis of the  $^{13}\text{C}$  hyperfine tensor, and should perhaps stress here that these coefficients are expected to have opposite signs for the phase choice in Fig. 6.6, so that the unpaired electron density on the carbon is out along the external bisector of the OCO angle. As we have already remarked, the decrease in  $g_{YY}$  from the free spin value suggests that we need an excited state with considerable  $p_x$  character and from Table 6.5 we see that a  $b_1$ -orbital would be appropriate. According to the level scheme the first vacant orbital has this symmetry so the excited state should be relatively low in energy and perhaps dominate the contributions to  $g_{YY}$ . We will take the orbital to be

$$\psi_{b_1} = c'_{xc}p_x + c'_{xo}(p_{x1} + p_{x2}) \quad (6.68)$$

using primes to associate coefficients with the excited state.

We now use (6.67) and (6.68) in (6.64). Putting in the LCAO expansions and taking the coefficients to be real gives

$$g_{YY} = g_e - (2/\Delta)\{c_{xc}c'_{xc}\zeta_C\langle p_x|l_y|p_x\rangle + c_{xo}c'_{xo}\zeta_O\langle p_{x1} + p_{x2}|l_y|p_{x1} + p_{x2}\rangle\} \\ \times \{c'_{xc}c_{xc}\langle p_x|l_y|p_x\rangle + c'_{xo}c_{xo}\langle p_{x1} + p_{x2}|l_y|p_{x1} + p_{x2}\rangle\} \quad (6.69)$$

where the  $\Delta$  is the difference of orbital energies shown in Fig. 6.7. The matrix elements are given in Table 6.1, and putting in their values we obtain

$$g_{YY} = g_e - (2/\Delta)\{c_{xc}c'_{xc}\zeta_C + 2c_{xo}c'_{xo}\zeta_O\}\{c'_{xc}c_{xc} + 2c'_{xo}c_{xo}\} \quad (6.70)$$

This expression illustrates the difficulties we mentioned about interpreting  $g$ -factor shifts: there are several unknowns and only one measured quantity.

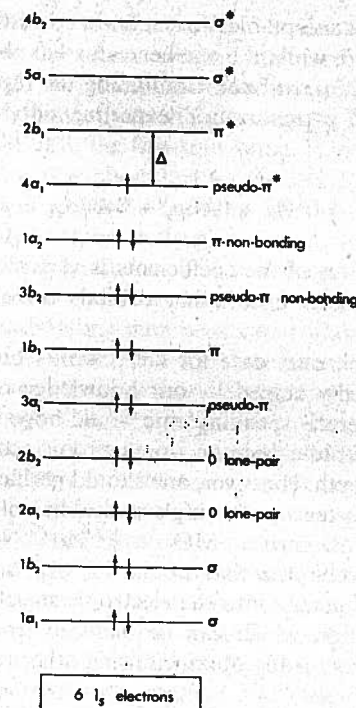


FIG. 6.7. The molecular orbital level scheme for  $\text{CO}_2^-$  [138]. Antibonding orbitals are starred; the pseudo- $\pi$ -orbitals correlate with  $\pi$ -orbitals of linear  $\text{CO}_2$ . No attempt has been made to indicate relative energies.

We will try to estimate  $c_{xo}$ , to check our remark that the coefficients of the other oxygen orbitals in the singly occupied orbital are small, and to complete our estimate of the singly occupied orbital. We take  $c_{xc} = 0.66$  from our analysis of the  $^{13}\text{C}$ -tensor in Section 4.4. For the atomic orbital coefficients in the excited state we use the values adopted by Ovenall and Whiffen [138]. They took  $c'_{xc} = 0.75$ ,  $c'_{xo} = -0.47$ , these being renormalised values for the corresponding coefficients calculated for  $\text{NO}_2$  by Mulligan [211]. The optical spectrum of  $\text{CO}_2^-$  in irradiated formate crystals has been analysed by Chantry and Whiffen [212], and the longest wavelength absorption at  $29,400\text{ cm}^{-1}$  assigned to the  $2b_1 \leftarrow 4a_1$  transition, so we use this value for  $\Delta$ . With the standard values of  $28\text{ cm}^{-1}$  and  $152\text{ cm}^{-1}$  respectively for  $\zeta_C$  and  $\zeta_O$ , solution of the quadratic for  $c_{xo}$  obtained from (6.70) gives

$$c_{xo} = +1.07 \text{ or } -0.44 \quad (6.71)$$

The larger value is not acceptable, since it is not consistent with normalisation of the  $4a_1$ -orbital, while the smaller value has the sign expected for the antibonding pseudo- $\pi$ -orbital. Combining the results of the analyses of the hyperfine and  $g$ -tensors our 'experimentally' determined singly occupied orbital is

$$\psi_{4a_1} = 0.39s + 0.66p_z - 0.44(p_{z1} + p_{z2}) \quad (6.72)$$

The sum of the squares of the coefficients is very close to unity, so our claim that contributions from other orbitals on oxygen are small is supported.

The analysis of the e.s.r. data for  $\text{CO}_2^-$  works out very well indeed, though it is admittedly helped by our knowledge of the much-studied  $\text{NO}_2$  molecule. Generally speaking, one would hope to be able to understand the spectra of radicals in an iso-electronic sequence to about the same quantitative depth. However, one should perhaps be more cautious about analysing the  $g$ -tensor of a single radical in isolation, and not place too much reliance on derived MO coefficients. Notwithstanding any reservations, it should be clear that the analysis of  $g$ - and hyperfine-tensors gives a great deal of insight into the electronic structure of radicals. The amount of information which can be deduced from the e.s.r. is very impressive, and not as readily obtained using other techniques.

## 6.7 Aromatic Radicals

The result (6.64) can be used to calculate the  $g$ -tensor of any doublet molecule and Stone [213] has shown how the expression may be developed for the particular case of conjugated  $\pi$ -radicals. In this section we review this theory.

Compared to the hyperfine splitting, the  $g$ -tensor and  $g$ -factors of aromatic radicals have received comparatively little attention. It is not difficult to see why. The anisotropy of the  $g$ -tensor of an aromatic radical is expected to be fairly small, so that even if oriented samples can be prepared it is difficult to measure accurately since the complex hyperfine structure makes the spectra poorly resolved, the linewidths in solids being often comparable to the hyperfine splittings [214]. In contrast the  $g$ -factors can be measured from solution spectra with high precision, though this has not generally been done as a matter of routine, presumably because of the effort required to interpret the results.

The  $g$ -tensors of  $\pi$ -radicals were first discussed, qualitatively, by McConnell and Robertson [215] who offered an explanation of why the  $g$ -factors observed were higher than the free spin value, the shift being

greater for semiquinone ions than for hydrocarbon ions. Their argument is easy to follow if we think for a moment about a C—H fragment, calling the axis of the singly occupied  $2p$ -orbital the  $z$ -direction. This orbital cannot mix with anything which will give angular momentum about the  $z$ -axis, so  $g_{zz}$  should have the free-spin value. However in the  $x$ - $y$ -plane the admixture of  $p_x$  and  $p_y$  should cause the  $g$ -factor to deviate from  $g_e$ . The orbitals involved are the  $\sigma$ -bonding orbitals, which lie below  $2p_z$  (or  $\pi$ ), and are doubly occupied in the groundstate, and the  $\sigma^*$  antibonding orbitals, which lie above  $2p_z$  and are empty in the ground state. One would expect the  $\sigma^*$ -orbitals to be further from  $2p_z$  in energy since antibonding orbitals are more antibonding than bonding orbitals are bonding, so that the  $\sigma$ -orbitals would be admixed to a greater extent. Thus, since the more important excited states would be those in which an electron was promoted into the formally singly occupied orbital the  $g$ -factors should be greater than the free-spin value. In the case of substituted radicals, such as semiquinones, one would have to take into account excitations from  $\sigma$ -lone-pair orbitals which should lie much closer in energy to the singly occupied orbital so that there should be larger deviations of the  $g$ -factors from the free-spin value. These ideas afforded a satisfactory qualitative explanation of the trend of the observed  $g$ -factors, and were further supported when studies of aliphatic radicals trapped in single crystals were started. As we have seen in Chapter 4, the spectra of these are relatively simple so the  $g$ -tensor can be measured quite precisely, and these radicals provide good models for the aromatic fragment. For example, the radical  $\text{CH}(\text{OH})\text{COOH}$  in glycolic acid has  $g_z = 2.0017$ , while the in-plane elements are 2.0053 and 2.0038 [152].

Stone's theory [213] uses these ideas quantitatively, and obtains the  $g$ -tensor of an aromatic radical by summing contributions from all the C—H and C—C bonds. We first consider the calculation of the  $g$ -factor for such a radical, and will use the axis system shown in Fig. 6.8. For the C—C fragment, the relevant part of the singly occupied  $\pi$ -orbital can be written as

$$\psi_\pi = c_1 p_{z1} + c_2 p_{z2} \quad (6.73)$$

while for the bond we have

$$\psi_b = (1/\sqrt{6})\{(s_1 - \sqrt{2}p_{y1}) + (s_2 + \sqrt{2}p_{y2})\} \quad (6.74)$$

with the antibonding orbital

$$\psi_a = (1/\sqrt{6})\{(s_1 - \sqrt{2}p_{y1}) - (s_2 + \sqrt{2}p_{y2})\} \quad (6.75)$$



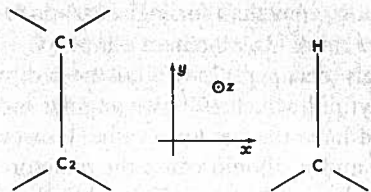


FIG. 6.8. Local axes for calculating the  $g$ -tensor contributions from C—C and C—H bonds in an aromatic radical.

Using these forms in (6.64) we obtain

$$g_{ZZ}^{CC} = g_Y^C = g_e$$

$$g_{XX}^{CC} = g_e + \frac{2(c_1 + c_2)^2 \zeta_C}{E_\pi - E_a} + \frac{2(c_1 - c_2)^2 \zeta_C}{E_\pi - E_b} \quad (6.76)$$

where  $E_\pi$ ,  $E_a$  and  $E_b$  are the energies of the  $\pi$ , antibonding, and bonding orbitals respectively. The contribution to the  $g$ -factor is

$$\langle g \rangle^{CC} = g_e + \frac{1}{3} g_{XX}^{CC} \quad (6.77)$$

For the C—H fragment the relevant orbitals are

$$\psi_\pi = c p_z \quad (6.78)$$

$$\psi_b = 1/\sqrt{2} \{ c_1 [(1/\sqrt{3})s + (\sqrt{2}/3)p_z] + c_2 h \} \quad (6.79)$$

$$\psi_a = 1/\sqrt{2} \{ c_2 [(1/\sqrt{3})s + (\sqrt{2}/3)p_z] - c_1 h \} \quad (6.80)$$

where  $h$  denotes the hydrogen  $1s$ -orbital. The contributions to the elements of the  $g$ -tensor are

$$g_{YY}^{CH} = g_{ZZ}^{CH} = g_e \quad (6.81)$$

$$g_{XX}^{CH} = g_e + \frac{2c^2 c_1^2 \zeta_C}{E_\pi - E_b} + \frac{2c^2 c_2^2 \zeta_C}{E_\pi - E_a} \quad (6.82)$$

and the contribution to the  $g$ -factor is analogous to (6.77).

In order to compare  $g$ -factors of different molecules Stone [213] suggested developing (6.76) and (6.82) by writing  $E_\pi$  as the Hückel energy,

$$E_\pi = \alpha + \lambda\beta \quad (6.83)$$

and then expanding in powers of  $\lambda$ , thus one obtains

$$\langle g \rangle^{CC} = g_e + (c_1 + c_2)^2 (\gamma_1 + \lambda\gamma'_1) + (c_1 - c_2)^2 (\gamma_2 + \lambda\gamma'_2) + \dots \quad (6.84)$$

and

$$\langle g \rangle^{CH} = g_e + c^2 (\gamma_3 + \lambda\gamma'_3) + \dots \quad (6.85)$$

By collecting terms about particular atoms, it is possible to express the  $g$ -factor contributions for each atom as functions of  $\lambda$  similar in form to (6.84) and (6.85). For a carbon atom bonded to three others one obtains, to first order in  $\lambda$ ,

$$\langle g \rangle^{C_i} = g_e + 3c_i^2 \{ (\gamma_1 + \gamma_2) + \lambda(\gamma'_1 + \gamma'_2) \} + c_i(c_j + c_k + c_l) \{ (\gamma_1 - \gamma_2) + \lambda(\gamma'_1 - \gamma'_2) \} \quad (6.86)$$

where  $c_i$  is the coefficient of the atom in question in the singly occupied orbital and  $c_j$ ,  $c_k$  and  $c_l$  are those of its neighbours. These latter coefficients can be eliminated using the Hückel secular equation

$$(\alpha - E_\pi)c_i + \beta(c_j + c_k + c_l) = 0, \quad (6.87)$$

with (6.83) to give

$$(c_j + c_k + c_l) = \lambda c_i \quad (6.88)$$

Substituting in (6.86) and again dropping second-order terms in  $\lambda$  gives

$$\langle g \rangle^{C_i} = g_e + c_i^2 \{ 3(\gamma_1 + \gamma_2) + \lambda(3\gamma'_1 + 3\gamma'_2 + \gamma_1 - \gamma_2) \} \quad (6.89)$$

Similarly for a carbon atom bonded to two others and to a hydrogen one obtains

$$\langle g \rangle^{C_j} = g_e + c_j^2 \{ (2\gamma_1 + 2\gamma_2 + \gamma_3) + \lambda(2\gamma'_1 + 2\gamma'_2 + \gamma_1 - \gamma_2) \} \quad (6.90)$$

Now if

$$\gamma_1 + \gamma_2 + \gamma_3 \quad \text{and} \quad \gamma'_1 + \gamma'_2 = \gamma'_3 \quad (6.91)$$

addition of all the contributions to the  $g$ -factor gives the result

$$\langle g \rangle = g_e + 3(\gamma_1 + \gamma_2) + \lambda(3\gamma'_1 + 3\gamma'_2 + \gamma_1 - \gamma_2) \quad (6.92)$$

by using the normalisation condition

$$\sum_i c_i^2 + \sum_j c_j^2 = 1 \quad (6.93)$$

Thus we can write for the departure of the  $g$ -factor from the free spin value, the  $g$ -shift,

$$\Delta\langle g \rangle = b + c\lambda \quad (6.94)$$

so the final result is the prediction of a very simple relationship between the  $g$ -shift and the Hückel energy of the singly occupied orbital. Stone [213] tested (6.94) on the then available data for hydrocarbon ions and found no significant deviation from linearity for the 11 data points. The least squares fit gave  $b = (24.7 \pm 0.8) \times 10^{-5}$ ,  $c = -(19.3 \pm 2.4) \times 10^{-5}$ . It is interesting to note that the intercept  $b$  should be the  $g$ -shift for neutral

odd-alternant radicals in which the unpaired electron occupies a non-bonding orbital for which  $\lambda = 0$ .

Segal, Kaplan and Fraenkel [216] made a more stringent test of (6.94) by re-measuring  $g$ -factors for 16 hydrocarbon ions to very high precision. They found that the  $g$ -factors of orbitally non-degenerate radicals fitted Eq. (6.94) extremely well, with  $b = (31.9 \pm 0.4) \times 10^{-5}$ ,  $c = (16.6 \pm 1.0) \times 10^{-5}$ . The  $g$ -factors of the orbitally degenerate ions benzene, coronene, and cyclooctatetraene, did not fall on the line and were not used in obtaining  $b$  and  $c$ . This behaviour is not unexpected in view of the orbital degeneracy, but as yet there has been no simple theoretical treatment of the  $g$ -factors of these ions.<sup>†</sup> The  $g$ -shift for triphenyl methyl and perinaphthyl were somewhat different from  $b$ , but the shift for perinaphthyl was noted to be solvent-dependent. The overall conclusion from these investigations is that Stone's theory gives a very good account of the  $g$ -factors of non-degenerate hydrocarbon ions. This is an impressive achievement, especially when one recalls that it uses a Hückel description of the electronic structures of the radicals.

The  $g$ -factors of semiquinone anions were also predicted by Stone to obey equations analogous to (6.94), and this prediction was confirmed for a small number of data points. There does not appear to have been any other major discussion of the  $g$ -factors of other types of aromatic radical.

Stone later considered the calculation of the actual  $g$ -tensors for hydrocarbon radicals [217]. The tensor can be expressed as a sum of terms from each atom, but of course these have to be referred to a molecular axis system before they can be summed. There are also two further terms to consider, arising from the coupling of the spin of the unpaired electron to its own 'ring current' motion induced by the magnetic field, and to the ring current due to all the other electrons. Stone calculates these terms explicitly, and finds contributions of about  $6 \times 10^{-5}$  to the  $g$ -tensor elements. The overall predictions of the calculations depend on the values of some parameters which are not easily estimated, but some clear predictions do emerge. In particular, it is predicted that  $(g_{xx} - g_{yy})$  should be equal in magnitude but opposite in sign for the radical anion and radical cation of a particular hydrocarbon, the directions of the principal axes being the same in both. Neutral odd-alternant radicals are predicted to have  $g_{xx} = g_{yy} = 2.0027$ ,  $g_{zz} = 2.0024$ .

There have been no direct measurements of the  $g$ -tensors of aromatic radicals, so Stone's predictions have not been stringently tested. As we will see in Chapter 9 the  $g$ -tensor does appear in expressions for the linewidths in the spectra of radicals in solution and in principle it should be possible to extract  $g$ -tensor information from linewidth data. However, there are several complicating features of the linewidth analysis and it

<sup>†</sup> Benzene anion is now well-understood [464].

has not proved possible to obtain clear-cut  $g$ -tensor information. De Boer's [218] analysis for some hydrocarbons supports Stone's calculations of the signs of  $(g_{xx} - g_{yy})$  and shows that it does change sign between positive and negative ions. Glarum and Marshall [161] have measured  $g_{xx} = g_{yy} = 2.00278$ ,  $g_{zz} = 2.00226$  for perinaphthyl oriented in a liquid crystal: we have already remarked the solvent dependence of the  $g$ -factor of this radical, so these observations do not demand that Stone's theory be questioned.

## 6.8 Rare-Earth Metal Ions

In all the cases considered so far in this chapter we have been able to treat the spin-orbit coupling as a perturbation of the levels of the ion or atom whose gross features were determined by the effects of the crystal or ligand field distorting the levels of the free ion or atom, as determined by the simple electronic Hamiltonian, i.e. the Hamiltonian containing only kinetic and intra-atomic coulombic energy terms. In the case of the rare-earth and actinide elements the situation is different. The unpaired electrons in these elements occupy  $4f$ - and  $5f$ -orbitals and since there are closed shells of electrons,  $5s$  and  $5p$  for the rare-earths, outside these, they are rather well shielded from the crystal fields, whose effect is thus much smaller than that of the spin-orbit coupling. Accordingly, the most convenient way to calculate the Zeeman splittings in these ions is to consider the effect of the spin-orbit coupling first, and then the perturbation due to the crystal field, which may be comparable to the Zeeman splitting. If the calculations were done exactly, the order in which the different terms were considered would not matter, but in using perturbation theory it is sensible to consider terms in order of diminishing effect.

To illustrate the style of calculation we will go over the treatment of the  $Ce^{3+}$  ion in an axially symmetric environment. The theory was originally given by Elliott and Stevens [219] and a full account is also given by Abragam and Bleaney [23] who in addition review later experimental results. Carrington and Longuet-Higgins [220] and Orton [221] have given accounts of the theory, and ours will be at about the same level.

The  $Ce^{3+}$  ion has a single  $4f$ -electron, so the ground term is  $^2F$ . From an elementary qualitative knowledge of the effects of spin-orbit coupling, we would expect this term to split into  $^2F_{5/2}$  and  $^2F_{7/2}$  levels, which, since the shell is less than half full, should form a normal multiplet with  $^2F_{5/2}$  lying lowest. This is indeed the case: it is easy to show, either by diagonalising the matrix of

$$\mathcal{H} = \lambda L \cdot S \quad (6.95)$$

in an  $|M_L M_S\rangle$  basis, or by using the results of the general theory of spin-orbit coupling [8,207] that the  $^2F$  term splits to give six levels of energy



$-2\lambda$  and eight of energy  $+\frac{3}{2}\lambda$ . The separation,  $\frac{7}{2}\lambda$ , amounts to about  $2200 \text{ cm}^{-1}$  in the free ion, and since this is much larger than any crystal field splitting we only need to consider the  ${}^2F_{5/2}$  level in a first approximation. The six-fold degenerate states of  ${}^2F_{5/2}$  can be classified as eigenfunctions of  $\mathbf{J}^2$ ,  $J_z$ ,  $\mathbf{L}^2$ , and  $\mathbf{S}^2$  simultaneously. We will find the eigenvalue of  $J_z$  the most convenient label, and the functions  $|J_z\rangle$  are, in terms of the original  $|M_L M_S\rangle$  functions,

$$\begin{aligned} |+\frac{1}{2}\rangle &= \sqrt{\frac{4}{7}}|1, -\frac{1}{2}\rangle - \sqrt{\frac{3}{7}}|0, \frac{1}{2}\rangle \\ |-\frac{1}{2}\rangle &= \sqrt{\frac{4}{7}}|-1, +\frac{1}{2}\rangle - \sqrt{\frac{3}{7}}|0, -\frac{1}{2}\rangle \\ |+\frac{3}{2}\rangle &= \sqrt{\frac{5}{7}}|2, -\frac{1}{2}\rangle - \sqrt{\frac{2}{7}}|1, \frac{1}{2}\rangle \\ |-\frac{3}{2}\rangle &= \sqrt{\frac{5}{7}}|-2, +\frac{1}{2}\rangle - \sqrt{\frac{2}{7}}|-1, -\frac{1}{2}\rangle \\ |+\frac{5}{2}\rangle &= \sqrt{\frac{6}{7}}|3, -\frac{1}{2}\rangle - \sqrt{\frac{1}{7}}|2, \frac{1}{2}\rangle \\ |-\frac{5}{2}\rangle &= \sqrt{\frac{6}{7}}|-3, +\frac{1}{2}\rangle - \sqrt{\frac{1}{7}}|-2, -\frac{1}{2}\rangle \end{aligned} \quad (6.96)$$

We now have to consider the effect of the crystal field. For the  $d$ -group transition ions we were able to do this qualitatively, thinking in terms of electrostatic interactions involving the real forms of the  $d$ -orbitals. However that is not convenient here, for the real forms of the  $f$ -orbitals are unfamiliar and more complicated than the  $d$ -orbitals, and furthermore we would expect the functions (6.96) to be rather awkward when expressed in terms of the real forms. Instead we shall use the results of crystal field theory. It would be a long diversion for us to derive the result from scratch, so we will merely indicate in a general way how it arises, referring the reader to standard treatments for more detail [8, 23].

The crystal field is calculated as the electrostatic field of an array of point charges of the appropriate symmetry, and the potential is written as a sum of spherical harmonics. If one is considering the effect upon orbitals of particular  $l$  only the even spherical harmonics are required, and for  $f$ -electrons terms up to sixth order need, in general, to be retained. We will consider  $\text{Ce}^{3+}$  in the ethyl sulphate, where the ion occupies a site of  $C_{3h}$  symmetry, and then only second- and fourth-order terms are necessary if we work solely within the  $J = \frac{5}{2}$  level. The crystal field potential for this case is

$$V = A_2^0(3z^2 - r^2) + A_4^0(35z^2 - 30r^2z^2 - 3r^4) \quad (6.97)$$

To see how this splits up the  $J = \frac{5}{2}$  levels we note that this potential can be expressed in terms of an equivalent operator, which is a function of angular momentum operators. This is possible because one can construct from the

angular momentum operators which have the same transformation properties as the spherical harmonics. An equivalent operator to (6.97) is

$$\begin{aligned} \mathcal{H} = a_2\langle r^2\rangle\{3J_z^2 - J(J+1)\} + a_4\langle r^4\rangle\{35J_z^4 - 30J(J+1)J_z^2 \\ + 25J_z^2 - 6J(J+1) + 3J^2(J+1)^2\} \end{aligned} \quad (6.98)$$

The coefficients depend on the system under consideration and are calculated by evaluating matrix elements of (6.97) and (6.98) and comparing the results. Extensive tabulations of operator equivalents and numerical values of the coefficients are given by Abragam and Bleaney [23]. For our purpose it is sufficient to note that (6.98) contains no terms in  $J_x$  or  $J_y$ , so its matrix is diagonal in the basis of functions  $|J_z\rangle$ , (6.96). Thus the effect is to split the six-fold degenerate  $J = \frac{5}{2}$  level into three Kramers doublets having  $J_z = \pm\frac{1}{2}$ ,  $\pm\frac{3}{2}$ ,  $\pm\frac{5}{2}$ . The magnitude of the splitting and the order in energy of the doublets is determined by the crystal field. The splittings of the  ${}^2F$  term by the successive effects of the spin-orbit coupling and crystal field are illustrated in Fig. 6.9, where we have assumed that the  $J_z = \pm\frac{1}{2}$  doublet lies lowest.

Application of a magnetic field lifts the degeneracy of the doublets. As in the earlier examples we use the Hamiltonian (6.16) to calculate the splittings, but now we will assume that  $g_e$  is exactly 2. In the basis of the  $J_z = \pm\frac{1}{2}$  functions the matrix of the Hamiltonian is

$$\begin{array}{cc} & |+\frac{1}{2}\rangle & |-\frac{1}{2}\rangle \\ \langle +\frac{1}{2}| & +\frac{2}{7}\beta H_z & \frac{2}{7}\beta(H_x - iH_y) \\ \langle -\frac{1}{2}| & \frac{2}{7}\beta(H_x + iH_y) & -\frac{2}{7}\beta H_z \end{array} \quad (6.99)$$

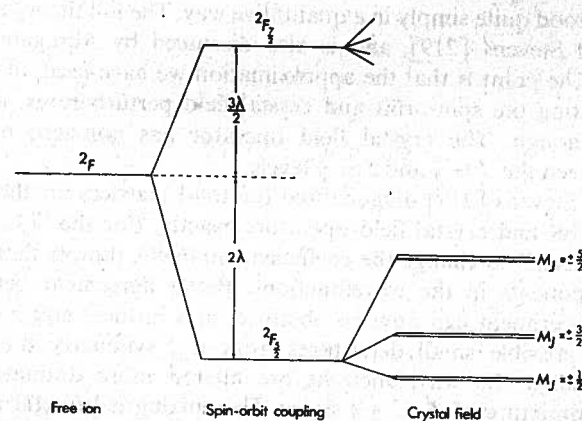


FIG. 6.9. Energy levels of an  $(f)^1$  ion in an axial crystal field.

Thus we obtain

$$g_{\parallel} = \frac{6}{7} (= 0.857); \quad g_{\perp} = \frac{18}{7} (= 2.571) \quad (6.100)$$

Experimentally [219],  $\text{Ce}^{3+}$  in lanthanum ethyl sulphate shows a resonance with  $g = 0.955$ ,  $g_{\perp} = 2.185$ , and this is assigned to the  $\Delta M_J = 1$  transition between the  $J_z = +\frac{1}{2}$  and  $J_z = -\frac{1}{2}$  levels. The agreement between the observed  $g$ -tensor, and that calculated using the above simple theory is quite good. Shortly we shall indicate the way in which the theory can be improved and better agreement obtained.

Before doing that however, we note the results of calculating the splittings of the  $J_z = \pm\frac{3}{2}$  and  $J_z = \pm\frac{5}{2}$  doublets. In the basis of the appropriate functions (6.96) the Zeeman operator is diagonal since  $L_{\pm}$  and  $S_{\pm}$  only have non-zero matrix elements between  $|M_L, M_S\rangle$  and  $|M_L \pm 1, M_S\rangle$  and  $|M_L, M_S \pm 1\rangle$ . Thus for both cases  $g_{\perp} = 0$ . The diagonal matrix elements give the values of  $g_{\parallel}$ , and the collected results are

$$J_z = \pm\frac{3}{2} \quad g_{\parallel} = \frac{18}{7} (= 2.571), g_{\perp} = 0 \quad (6.101)$$

$$J_z = \pm\frac{5}{2} \quad g_{\parallel} = \frac{30}{7} (= 4.286), g_{\perp} = 0 \quad (6.102)$$

We would not normally expect to observe the parallel transitions because of the  $\Delta M_J = \pm 1$  selection rule. However,  $\text{Ce}^{3+}$  in lanthanum ethyl sulphate shows, in addition to the resonance mentioned above for the  $J_z = \pm\frac{1}{2}$  doublet, a second resonance, in a state about  $3 \text{ cm}^{-1}$  above the ground state, with  $g_{\parallel} = 3.72$ ,  $g_{\perp} = 0.2$  [219], in fair agreement with expectation for the  $J_z = \pm\frac{5}{2}$  doublet, (6.102).

The departures of the  $g$ -tensors from the first-order values, and the non-zero transition probability for the resonance in the  $J_z = \pm\frac{5}{2}$  doublet can be understood quite simply in a qualitative way. The full theory is due to Elliott and Stevens [219], and is also discussed by Abragam and Bleaney [3]. The point is that the approximation we have used, of completely separating the spin-orbit and crystal field perturbations, is not quite good enough. The crystal field operator has non-zero matrix elements between the  $J = \frac{5}{2}$  and  $J = \frac{7}{2}$  levels.

Elliott and Stevens [219] diagonalised the total matrices for the sum of the spin-orbit and crystal field operators exactly. For the ' $J_z = \pm\frac{1}{2}$ ' doublet the effect is to change the coefficients in (6.96), though there are no new components in the wavefunctions. Better agreement between theory and experiment can now be obtained, and further improved by allowing for possible small departures from  $C_{3h}$  symmetry. For the ' $J_z = \pm\frac{5}{2}$ ' doublet the wavefunctions are altered more dramatically, there being admixture of  $J_z = \pm\frac{7}{2}$  states. This mixing is brought about by the sixth-order crystal field term, which we omitted from (6.97) as we

were concerned solely with a pure  $J_z = \pm\frac{5}{2}$  doublet. The matrix elements of  $J_{\pm}$  between the components of the improved ' $J_z = \pm\frac{5}{2}$ ' doublet are now non-zero and the transition is observable. Further,  $g_{\perp}$  is no longer zero, and of course  $g_{\parallel}$  is also modified. While this theory gives a good account of the spectrum of  $\text{Ce}^{3+}$  in lanthanum ethyl sulphate, we should also note that the second-order Zeeman interaction can mix components of different doublets derived from the  $J = \frac{5}{2}$  level and so make formally  $\Delta J_z > 1$  transitions weakly allowed.

The case of  $\text{Ce}^{3+}$  in lanthanum ethyl sulphate is rather unusual in that the crystal field splitting is sufficiently small for more than one state to be populated. However, the principles of the analysis we have sketched apply fairly generally for rare-earth ions. Analysis of the spectra, perhaps together with other data, for example, from magnetic susceptibility measurements, often enables one to build up a very clear picture of the electronic levels of the ion in a crystal [23].